scientific reports

Check for updates

OPEN

Biogenic silver nanoparticles optimization using Plackett–Burman design and its synergistic effect with cefotaxime against multidrug resistant clinical isolates

Hanzala Khan[1,2,3], Anum Gul[1,3]✉, Zainab Najam[1] & Taqdees Malik[2]

The rise in antibiotic resistance has created an urgent need for alternative strategies to combat multidrug-resistant (MDR) bacterial infections. Silver nanoparticles (AgNPs) possess unique antibacterial properties, making them a promising option in biomedical applications. This study explores the green synthesis of silver nanoparticles (AgNPs) using *Citrus sinensis* peel extract and their synergistic potential with cefotaxime against multidrug-resistant (MDR) clinical isolates. For the optimization of AgNPs synthesis, Plackett–Burman experimental design (PBD) was implemented that demonstrated incubation time, temperature and extract: $AgNO_3$ ratio as significant factors. The UV–Vis spectroscopy analysis revealed a characteristic absorbance peak of CS-AgNPs at 470 nm. The size of biosynthesized AgNPs was analyzed using Scanning Electron Microscopy (SEM), that showed size range of 50–60 nm with spherical shaped morphology. Fourier Transform Infrared Spectroscopy (FTIR) analysis found different functional groups involved in the stabilization and capping of AgNPs, as indicated by the peaks at 2925 cm^{-1}, 1630 cm^{-1}, 1100 cm^{-1} and 1016 cm^{-1} revealing –CH stretching aliphatic carbon, the carboxyl group, OH group and C–O–C group, respectively. The cytotoxicity of the synthesized CS-AgNPs and its synergistic effect with cefotaxime (CTX) antibiotic was analyzed with MTT assay. The combination of CS-AgNPs and CTX showed significant decrease in cytotoxicity compared to CS-AgNPs alone. Antibacterial activity of CS-AgNPs against MDR clinical isolates was performed using minimum inhibitory concentration (MIC) method. The MIC of CS-AgNPs was observed within 3.125–12.5 µg/ml range. Synergism assay of CS-AgNPs with CTX was also evaluated to determine the fractional inhibitory concentration (FIC) index. Clinical isolates (*E. coli*), S-11, S-14, S-16, S-19, and S-20 showed FIC in the range of 0.162–0.402 indicating synergism whereas, S-04, S-06, S-10, S-15 and S-21 showed the FIC in the range of 0.644–0.804 indicating the additive effect. The MDR *E. coli* clinical isolates S-11, S-16, S14, S-19 and S-20 demonstrated 65–85% biofilm inhibition which was significantly ($p \leq 0.001$) high in all tested isolates. Significant ($p \leq 0.001$) eradication of preformed biofilm in the range of 60–78% was also observed in S-16 clinical isolate.

Keywords Silver nanoparticles, *Citrus sinensis*, Green synthesis, Multi drug resistant (MDR), Cefotaxime (CTX), Antibacterial, Biofilm, Cytotoxicity

Antimicrobial resistance (AMR) is a major global health concern, affecting human health worldwide. As per global burden estimates, bacterial AMR was associated with approximately 4.95 million deaths worldwide in 2019, with 1.27 million deaths directly attributable to bacterial AMR[1]. The rise of multidrug-resistant (MDR) bacteria presents a significant global health challenge, particularly in underdeveloped regions where antibiotic overuse is widespread[2]. As a result, infections such as foodborne illnesses and pneumonia have become increasingly difficult to treat[3].

Bacteria have different mechanisms that contribute to the development of resistance against available antibacterial agents. Some of the mechanisms commonly found in bacteria are efflux pump, transportation of

[1]Dow College of Biotechnology, Dow University of Health Sciences, Karachi, Pakistan. [2]Department of Microbiology, Jinnah University for Women, Karachi, Pakistan. [3]Hanzala Khan and Anum Gul contributed equally to this work. ✉email: anum.gul@duhs.edu.pk; gul_anum@yahoo.com

genes and production of inactivating enzymes[4–7]. Additional approach adopted by microbes against antibiotic effect is the biofilm formation by which the penetration and diffusion of antibiotic is not easy[8–10]. Additionally, bacterial biofilm are capable to resist higher concentration of antibiotics in contrast to planktonic bacteria[6]. As bacteria are acquiring resistance rapidly, the development of improved antimicrobial compounds and alternative therapeutic approaches are urgently needed.

Nanotechnology is a rapidly growing research field which proves its potential as an alternative therapeutic approach. Recent literature shows that nanoparticles possess promising antibacterial potential against MDR bacteria that can be used alone or alongside existing antibiotics. Nanoparticles (NPs) are extensively used and have numerous applications in the healthcare, industries, diagnostics, and medicine[11]. Bacteria develop resistance by using multiple mechanisms due to which various antibiotics are no more effective in treating pathogenic infections[12]. Resistance towards nanoparticles has not been reported yet, therefore researchers are showing interest in the production of unique nanoparticles having antibacterial potential[13]. Nanoparticles range in size from 1 to 100 nm and exhibit antibacterial activity along with other unique physicochemical properties and also facilitate targeted drug delivery with increased effectiveness[14,15]. Several metals have been used recently in nanoparticle production like silver, platinum, gold, copper, and selenium[14]. Different synthesis methods, including physical, chemical, and biological, are being utilized to produce these nanoparticles. Among different approaches, the biological method is eco-friendly approach to produce NPs as compared to the other methods that uses toxic reactants and generates products with lethal and harmful side effects[16–18]. In biological approach, the synthesis of nanoparticles by using medicinal plants are broadly explored. During NPs synthesis, the phytochemicals found in the plants function as reducing, stabilizing, and capping agents, therefore contributing to different biological and medical applications. Among various nanoparticles, silver nanoparticles (AgNPs) have been highlighted for their effective antibacterial properties and are extensively used for coating on medical devices, preparation of wound dressings and gels[19].

Citrus sinensis, one of the citrus species, (commonly known as orange or sweet orange) is frequently used as fresh fruit or in the form of orange juice, and its peels contributes to approximately 50% of its weight[20]. *Citrus sinensis* have compounds like phenol and flavonoids which are reported for their antioxidant and antibacterial activities and are involved in the reduction and capping of the AgNPs[21–23]. AgNPs are powerful harmless antimicrobial compound that affect various microbes, even at lowest concentrations[24,25]. Silver nanoparticles with various shapes like spherical and hexagonal demonstrates significant antibacterial activity against MDR bacteria[26].

Optimization of AgNPs synthesis is also very important as various factors like temperature, time, pH, and concentration of $AgNO_3$ affect the synthesis method[27]. Optimization using single factor at a time approach takes a lot of time and increases the overall cost. In comparison to single factor optimization, the Design of experiment (DOE) approach is an efficient statistical program for randomized testing with optimization of two or more than two factors involved in the study design[28]. The total number of factors and levels of each factor are used to classify the design. This type of design permits the investigation of multiple factors eliminating the requirement of large number of trials[29]. It is a very efficient design that allows the collective optimization of all relating factors to overcome the challenges of single factor optimization method[30]. Optimization by DOE gives greater synthesis yield, lower variability in process and cut down overall cost[31]. Numerous studies have documented the optimization of AgNPs synthesis through the Plackett–Burman Design (PBD) of experiment[32].

The antibiotic Cefotaxime which belongs to third generation of cephalosporin is one of the most important antibiotics in treating various microbial infections[33]. However, there are various microbes that have developed resistance against this antibiotic through multiple mechanisms. In these resistance mechanisms, one mechanism is the production of beta lactamase enzyme by gram negative pathogens, specifically *E.coli*[34].The global increase in antibiotic resistance presents a considerable challenge, undermining the effectiveness of widely used antibiotics against prevalent bacterial infections. The 2022 Global Antimicrobial Resistance and Use Surveillance System (GLASS) report showed higher level of resistance among common bacterial pathogens. In 76 countries, the median resistance rates are concerning, with 42% of *E. coli* strains resistant to third-generation cephalosporin. This growing resistance is complicating the treatment of common infections[1]. According to the 2022 National Institute of Health (NIH) report, clinical isolates from laboratories across Pakistan identified *E. coli* as the most frequently reported pathogen, exhibiting 77% resistance to cefotaxime[35].

Therefore, based on the literature mentioned above, the aim of the study is to optimize the green synthesis of AgNPs using *Citrus sinensis* peel extract using Plackett–Burman Design and to evaluate its synergistic antibacterial and antibiofilm effects with cefotaxime. To the best of our knowledge. This study provides a novel approach by integrating green synthesis, statistical optimization, and synergistic antibacterial strategies to combat multidrug resistance. The combinatorial approach holds significant promise for enhancing the therapeutic potential of antibiotics against resistant pathogens, addressing the global challenge of antimicrobial resistance.

Results and discussion

The study focused on synthesizing and characterizing silver nanoparticles (CS-AgNPs) using *Citrus sinensis* peel extract and assessing their cytotoxicity, antibacterial and antibiofilm activity against MDR clinical isolates.

Factors which are involved in the synthesis were selected using PBD design of experiment which were used for the synthesis of AgNPs.

Optimization of CS-AgNPs synthesis using Plackett–Burman design (PBD)

Four factors (Incubation Time, Temperature, $AgNO_3$ conc and Ratio of plant extract to $AgNO_3$) were used for analysis. In this study, a total of 39 runs were generated using PBD from above mentioned four factors using statistical software Minitab 21 as shown in Table 1. The Plackett Burman design displayed vast differences in OD of CS-AgNPs at 470 nm. The lowest OD of CS-AgNPs was 0.079 whereas the highest OD was 1.461.

Run order	Incubation temperature	$AgNO_3$ concentration	Incubation time	Ratio of CS extract to $AgNO_3$	Mean OD	Standard Error of Mean (SEM)
1	50	5	0.5	10	0.097	0.006364
2	50	1	0.5	1	0.2255	0.003536
3	50	1	4	10	0.457	0.002828
4	50	1	4	1	0.7135	0.000707
5	30	5	4	10	0.6585	0.001414
6	50	1	4	1	0.634	0.011314
7	50	5	0.5	10	0.1105	0.001414
8	30	1	0.5	1	0.204	0.005657
9	30	1	0.5	1	0.209	0.023335
10	30	5	4	10	0.2035	0.002121
11	30	1	4	10	0.094	0.002121
12	30	5	0.5	1	0.2335	0.008485
13	50	1	4	1	0.5085	0.006364
14	30	5	4	10	0.1355	0.014849
15	50	1	0.5	1	0.239	0.002828
16	50	1	0.5	1	0.2285	0.002828
17	50	5	0.5	10	0.1135	0.009192
18	30	1	4	10	0.467	0.023335
19	30	5	4	1	0.4215	0.02687
20	50	5	0.5	10	0.1175	0.000707
21	50	5	4	1	1.3755	0.000707
22	30	5	0.5	1	0.2095	0.000707
23	50	1	4	10	0.369	0.009192
24	40	3	2.25	5.5	0.1105	0.000707
25	30	5	4	1	0.4215	0.001414
26	40	3	2.25	5.5	0.1015	0.012021
27	30	1	0.5	1	0.205	0.009192
28	40	3	2.25	5.5	0.1	0.001414
29	50	1	4	10	0.383	0.018385
30	30	5	0.5	1	0.2235	0.001414
31	30	1	0.5	10	0.0905	0.003536
32	30	1	4	10	0.083	0.006364
33	50	5	4	1	1.249	0.015556
34	50	5	4	1	1.461	0.001414
35	50	5	0.5	10	0.096	0.011314
36	30	1	0.5	10	0.074	0.002121
37	30	1	0.5	10	0.08	0.000707
38	30	5	4	1	0.573	0.001414
39	50	5	0.5	10	0.0975	0.000707

Table 1. Plackett Burman design (PBD) outcome.

The normal plot of standardized effects indicated the significance of the factors. Incubation time, temperature, and ratio of CS-extract to $AgNO_3$ were found to be significant factors at 95% confidence level whereas concentration of $AgNO_3$ was non-significant as shown in Fig. 1a.

The classification of factors that affect the AgNPs synthesis were analyzed by the Pareto chart. The Pareto chart showed three significant and one insignificant factor influencing the CS-AgNPs synthesis as represented in Fig. 1b.

In the normal probability plot as shown in Fig. 1c, the variables present adjacent to the straight line indicated that the data generated by Plackett Burman design showed normal distribution.

The main effect plot determined the effect of each factor at different levels in the synthesis of CS-AgNPs. The optimized values generated by the main effect plot included the 4 h of reaction incubation time which led to the maximum synthesis than the 0.5 and 2.25 h, the extract: $AgNO_3$ ratio of 1:1 resulted in the maximum synthesis rate as compared to the 1:5 and 1:10 ratio. The incubation temperature of 50 °C and 5 mM $AgNO_3$ concentration also showed the highest effect on the synthesis of CS-AgNPs as shown in Fig. 1d. The study by Oviedo et al. also reported similar findings that increasing the temperature till 50 °C increased the AgNPs synthesis[36]. Moreover, study by Ali et al. reported that AgNPs synthesis was improved when a mixture of silver nitrate and plant extract was used in equal ratio[37].

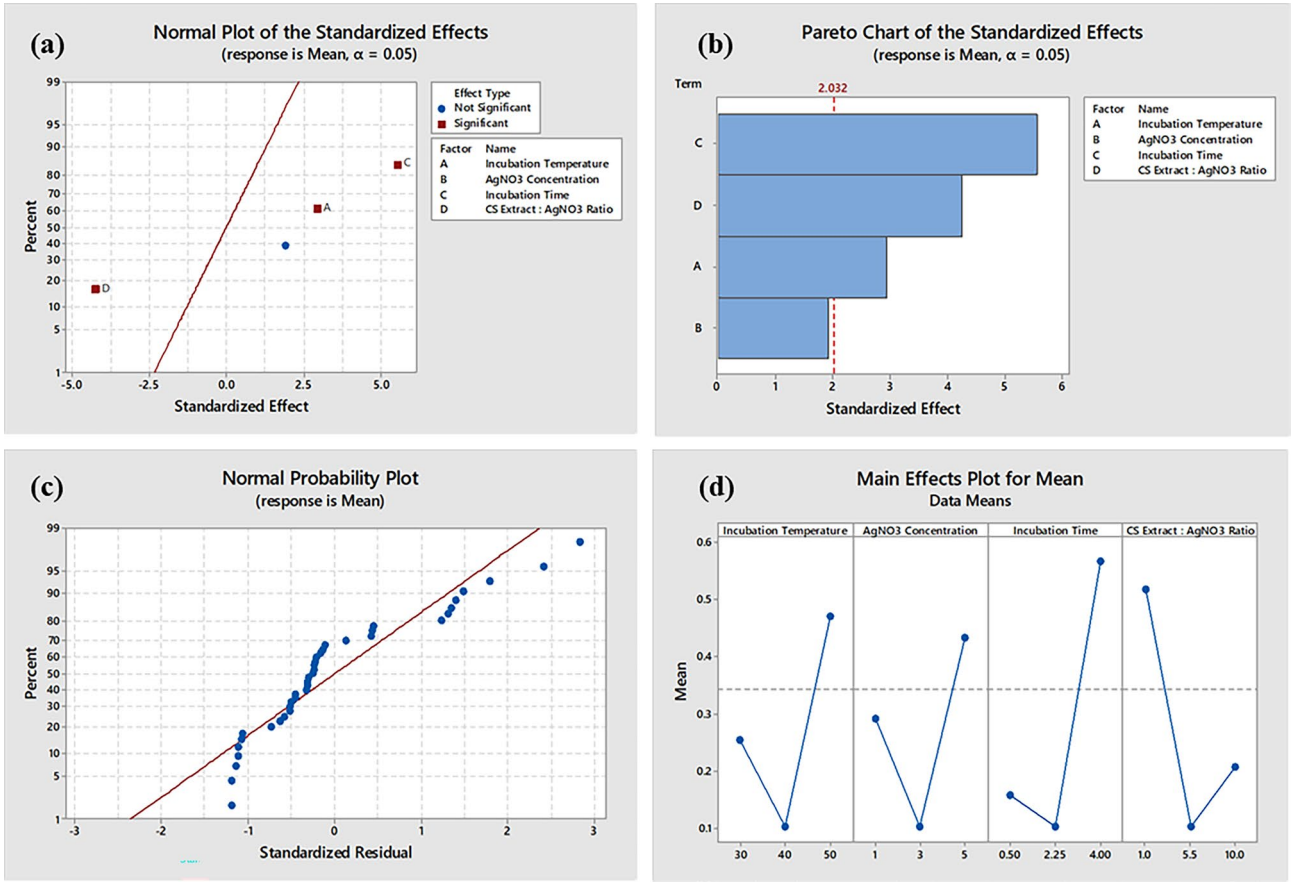

Fig. 1. Plackett–Burman Experimental Design Plots. (a) Normal plot of Standardized Effects. (Response is OD 470, α = 0.05). (**b**) Pareto Chart of Standardized Effects. The size of the bar shows their influence in the CS-AgNPs synthesis. (**c**) Normal Probability Plot. Plot shows the normal distribution of the data generated by the Plackett Burman design analysis. (**d**) Main Effect Plot. The plot indicates the effect of all four parameters on synthesis.

Synthesis of CS-AgNPs

The biosynthesis of CS-AgNPs was achieved by mixing the peel extract of *Citrus sinensis* with silver nitrate according to the optimized parameters following PBD analysis (Fig. 2a) Following the incubation period, the appearance of brown color indicated that CS-AgNPs had been synthesized, as depicted in Fig. 2b. The increase in incubation time resulted in the better CS-AgNPs synthesis that can be identified with the color change from light yellow to brown as a result of excitation of surface plasmon vibration[38]. Similar results have been reported in the literature where change in color from yellow to brown was observed as indicative of successful AgNPs synthesis[39,40].

Characterization of *Citrus sinensis* silver nanoparticles

UV–Vis spectroscopy of CS-AgNPs

A peak in the range of 400–500 nm confirmed the synthesis of AgNPs, with maximum absorbance recorded at 470 nm. The overlapping spectra of silver nitrate, CS-extract and synthesized CS-AgNPs are represented in Fig. 3. A similar surface plasmon resonance (SPR) peak was reported in previous studies that showed typical SPR peak for spherical AgNPs between 400 and 500 nm[39,41–43].

Scanning electron microscopy (SEM) and energy dispersive X-ray spectroscopy (EDX)

The SEM analysis reported circular shaped CS-AgNPs, with average size of 50-60 nm. Previous studies have reported the synthesis of AgNPs with similar size and shape. For instance, Mittal et al. synthesized spherical AgNPs (30–50 nm) from leaf extract of *Tinospora cordifolia*, while Margarita et al. reported ~ 50 nm AgNPs synthesized from orange peel extract, corroborating the findings of this study[44,45].

In EDX, further confirmation of nanoparticles formation was done by identifying the presence of elemental silver. A sharp peak of silver was observed at 3 keV in EDX as shown in Fig. 4. This confirmed the presence of CS-AgNPs as silver typically shows this specific peak at 3 keV[45,46].

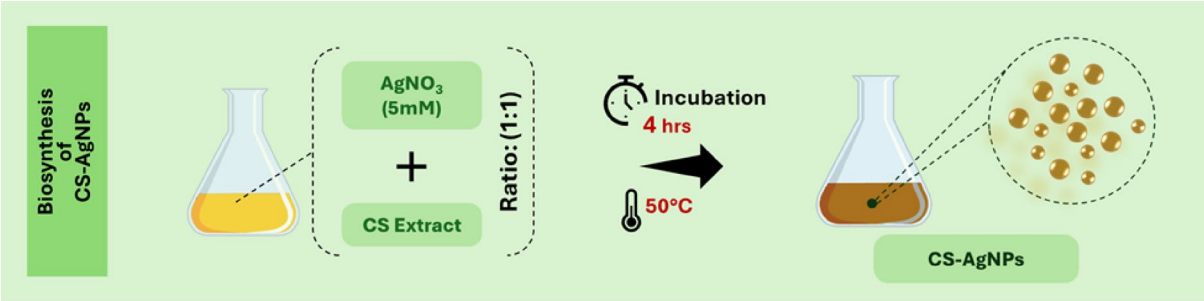

(a)

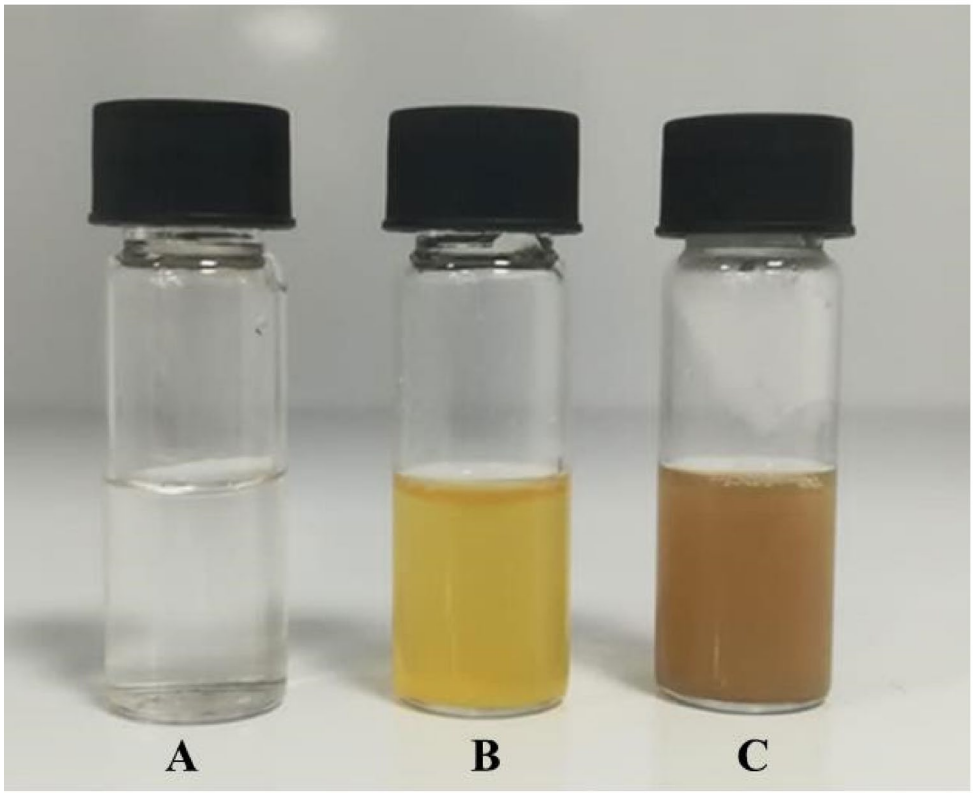

(b)

Fig. 2. (**a**) Biosynthesis of CS-AgNPs. (**b**) Synthesis of CS-AgNPs. (A) Silver nitrate solution (B) CS-Extract (C) Synthesized AgNPs after 4 h incubation.

Fourier transform infrared spectroscopy (FTIR)

Various peaks were generated by FTIR which were similar in both CS-extract and CS-AgNPs. The peak at 2925 cm^{-1} indicated –CH stretching of aliphatic carbon, 1630 cm^{-1} indicated the carboxyl group, 1100 cm^{-1} revealed the -OH group and 1016 cm^{-1} represents C–O–C as shown in Fig. 5. The identification of similar functional groups in AgNPs spectra demonstrated the involvement of these groups in stabilization and capping of AgNPs. These outcomes are in line with the findings from earlier studies that reported the presence of carboxyl and phenol functional groups in orange peels[47,48].

Cytotoxicity assay

The cytotoxic effect of tested compounds were interpreted as per ISO 10993-5:2009 standard guidelines, according to which the cell viability ≤ 70% is considered as a cytotoxic effect[49]. The cytotoxic effect of CS-AgNPs, CTX and their synergistic treatment against normal fibroblast cells were represented in Fig. 6. The results demonstrated that the viability of cells decreased with increasing concentration of CS-AgNPs, whereas CTX showed decreased toxicity with increased concentration (Fig. 6a). However, the combination treatment showed that the combination 3, 4, 5, 6, and 7 have synergistic effect showing decrease in cytotoxicity as compared to CS-AgNPs alone at respective concentrations (Fig. 6b).

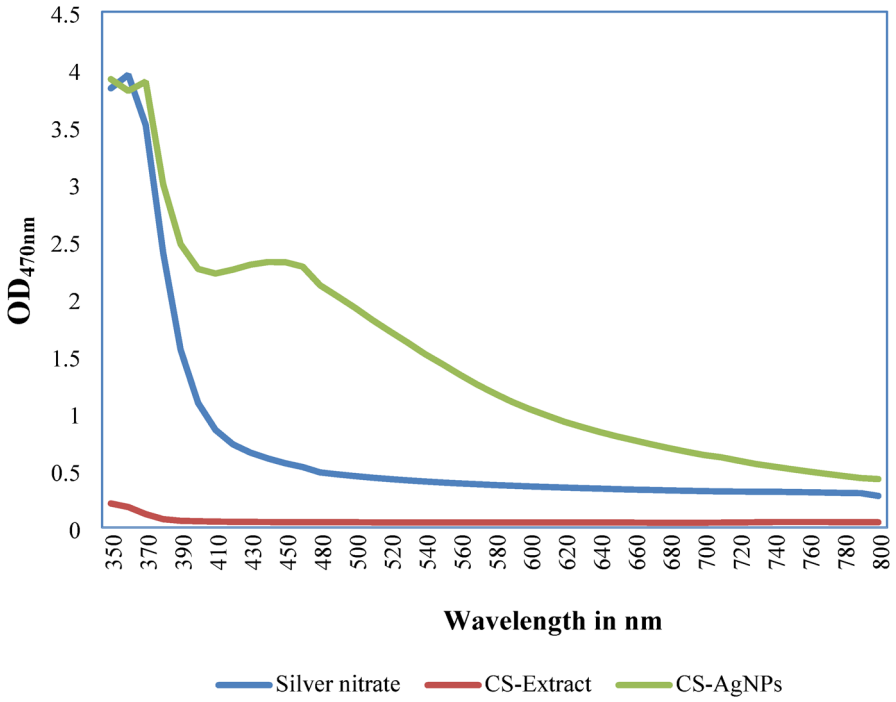

Fig. 3. UV/Vis spectra: The overlapping spectra shows blue, red and green lines representing the spectra of CS extract, silver nitrate and synthesized AgNPs. The CS-AgNPs showed maximum absorbance at 470 nm.

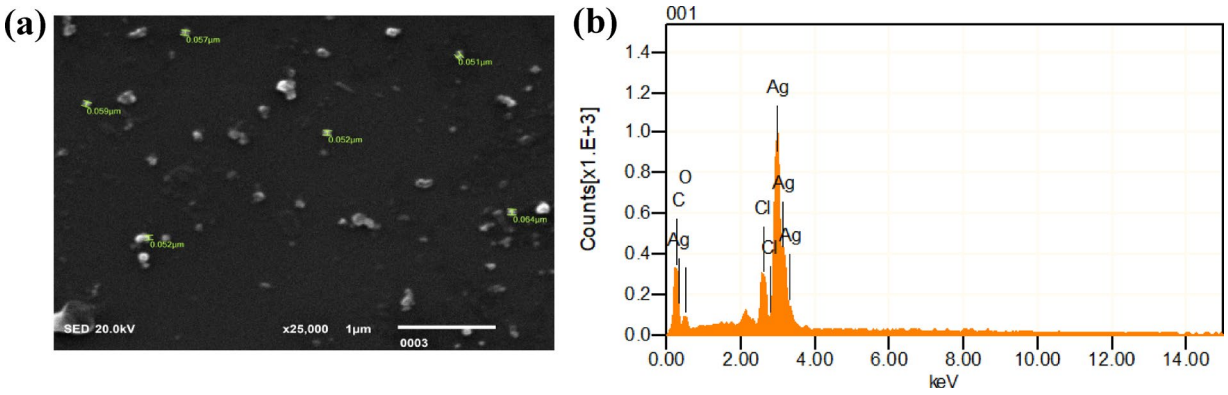

Fig. 4. SEM–EDX analysis of CS-AgNPs. (**a**) SEM Analysis of CS-AgNPs shows the spherical shaped and smaller size NPs. (**b**) EDX of CS-AgNPs indicating the sharp peak of silver at 3 keV.

Characterization of clinical Isolates

All clinical isolates were identified on selective and differential media, followed by gram staining, microscopy, and biochemical characterization. Out of twenty-three isolates, two isolates showed golden yellow color colonies on MSA media plate due to Mannitol salt fermentation by the bacteria that represented the presence of *Staphylococcus aureus* (Supplementary file).On MacConkey media, two isolates showed large pink color mucoid colony, indicative of the presence of *Klebsiella pnuemoniae* (Supplementary file). Only one isolate showed pink color colonies on MacConkey agar due to the utilization of lactose present in the medium which indicated the presence of *Enterobacter* (Supplementary file). On Eosin Methylene Blue (EMB) agar, the fermentation of lactose leads to the production of acid, which causes the eosin dye to combine with the methylene blue indicator, resulting in a characteristic green metallic sheen. Eighteen isolates showed green metallic sheen on EMB plates which is the characteristic property of *E. coli* (Supplementary file). Biochemical test results indicated that the predominant clinical isolates were *S. aureus*, *Klebsiella pnuemoniae, Enterobacter* and *E. coli.*

Antibiotic susceptibility of clinical isolates

Before the initiation of nanoparticles assays against MDR, it was important to validate the sensitivity pattern of the isolates. Following CLSI (2020) standard guidelines, antibiotic susceptibility testing was performed using the

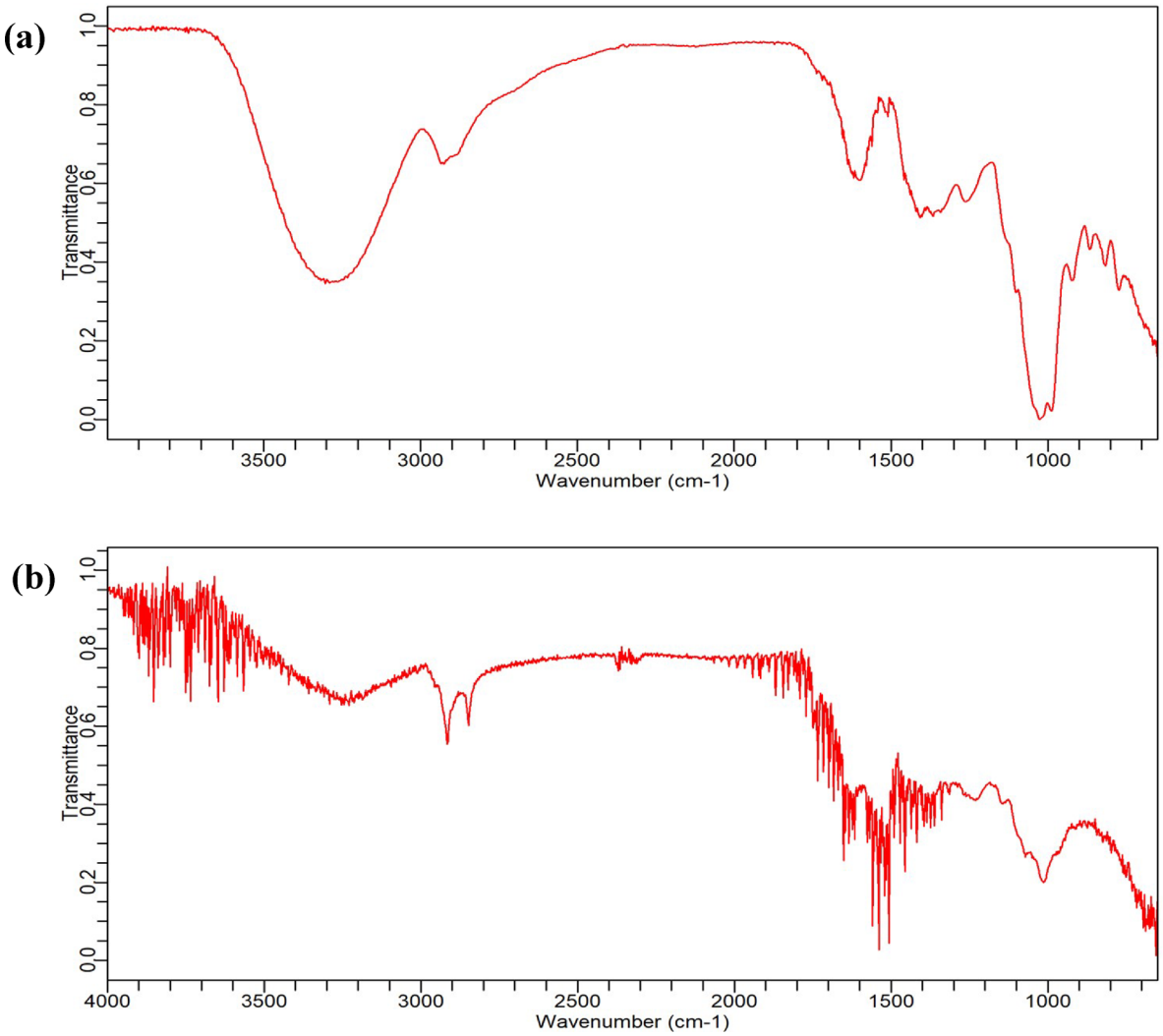

Fig. 5. FTIR spectra. The figure shows the peaks of different functional groups in (**a**) *Citrus Sinensis* (CS) extract and (**b**) AgNPs synthesized by the reduction of silver nitrate with the *Citrus sinensis*.

disc diffusion method. After incubation, plates were observed for clear zone around the disc and the diameter of inhibition zone was measured. The resulted data was then reported as sensitive, intermediate, and resistant as shown in Table 2. Out of twenty-three isolates (S1-S23), a total of twenty-one (91%) isolates were MDR strains and two were non MDR strains. Results of antibiotic susceptibility are shown in Fig. 7.

In our study multidrug resistance in *E. coli* has been reported similar to the research work done in Indus hospital, Karachi[50]. In 2018, a report published on antimicrobial resistance in Pakistan mentioned that the major challenges that contribute to the resistance of available therapeutic options include the collection of irrelevant registered product, inaccurate advertisement, wrong antibiotic prescription, self-medication and preference of valuable broad spectrum drug[51]. A study conducted at National Medical Center on antibiotic susceptibility pattern of pathogen reported that the Gram negative *E.coli* was the most frequently isolated bacteria in different diagnostic specimens[52].

Antimicrobial activity of AgNPs

Minimal inhibitory concentration (MIC) of CS-AgNPs

Among twenty one MDR clinical isolates, nine isolates (S-02, S-04, S-06, S-07, S-10, S-15, S-16 S-17, and S-21) showed lowest MIC value of 3.125 µg/ml of CS-AgNPs, whereas six clinical isolates (S-01, S-05, S-08, S-11, S-14 and S-19) were inhibited by 6.25 µg/ml concentration of CS-AgNPs and only five clinical isolates (S-03, S-09, S-13, S-18 and S-20) showed MIC value of 12.5 µg/ml among all the tested concentrations of CS-AgNPs (Table 3). The results demonstrated that Gram negative bacteria exhibit greater susceptibility to AgNPs in contrast to gram positive bacteria. Similar outcomes were observed in a study conducted with *Cannabis sativa* mediated AgNPs[53]. In Gram negative bacteria, presence of thin cell membrane and negatively charged lipopolysaccharide layer favors the AgNPs adherence and penetration inside the cell. In contrast to this, the thick cell wall in Gram-positive bacteria hinder their interaction with AgNPs[54–57]. The presence of functional groups on the AgNPs surface like phenol and aromatic compounds from the CS extract may also be involved in the potential

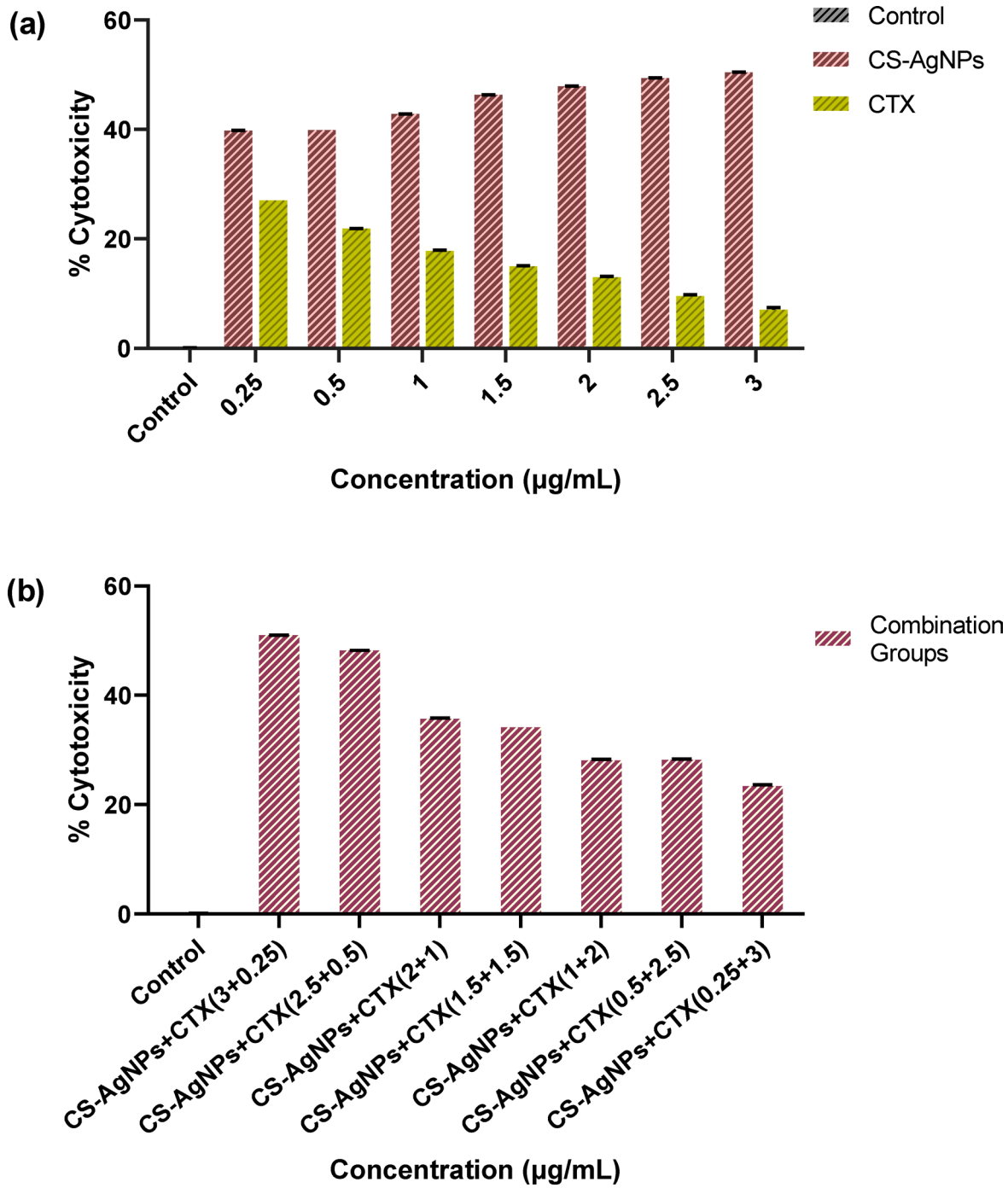

Fig. 6. Cytotoxicity Analysis. The graph shows cytotoxic effect of (**a**) CS-AgNPs and CTX and (**b**) their synergistic effect on BJ cell line.

antibacterial and antibiofilm activities of CS-AgNPs. These phytochemicals can be associated with CS-AgNPs stabilization. The study by Onitsuka et al. reported that the antimicrobial activity of the AgNPs was enhanced due to the polyphenols present in the plant extracts that work as reducing and stabilizing agents[58].

Minimum inhibitory concentration (MIC) of cefotaxime

The four isolates S-04, S-06, S-15, and S-16 showed bacterial inhibition at lowest concentration of 125 µg/ml CTX, whereas the isolates, S-10, S-11, S-19, and S-21 were inhibited by 250 µg/ml CTX. Only two isolates S-14 and S-20 showed inhibition at 500 µg/ml concentration and S-17 and S-05 showed complete inhibition against all concentrations (125, 25, 500 and 1000 µg/ml). In rest of the clinical isolates (S-01, S-02, S-03, S-05, S-07, S-08, S-09, S-12, S-13, and S-18), MIC was not observed at all the tested concentrations of CTX (Table 3).

Clinical isolates		Antibiotic sensitivity of clinical isolates (R = Resistant, I = Intermediate, S = Sensitive)												
strain	Code	AMP (10 µg)	AMC (30 µg)	AMK (30 µg)	GEN (10 µg)	CFM (5 µg)	CIP (5 µg)	IPN (10 µg)	CRO (30 µg)	NOR (10 µg)	CTX (30 µg)	AZM (15 µg)	SXT (10 µg)	VAN (30 µg)
E. coli	S 01	R	R	S	S	R	R	S	R	R	R	–	R	–
Enterobacter aerogenes	S 02	S	S	S	R	R	S	S	R	S	R	–	R	–
E. coli	S 03	R	S	S	S	R	R	S	R	R	R	–	S	–
E. coli	S 04	R	S	S	S	S	R	S	S	S	R	–	R	–
S. aureus	S 05	R	R	–	S	R	S	–	–	–	S	R	–	S
E. coli	S 06	R	S	S	S	S	R	S	S	S	R	–	R	–
K. pnuemoniae	S 07	R	R	S	S	R	R	S	R	R	R	–	R	–
	S 08	R	S	S	S	R	S	S	R	S	S	–	S	–
E. coli	S 09	R	S	S	S	R	S	S	R	S	R	–	S	–
	S 10	R	S	S	S	R	S	S	S	S	R	–	R	–
	S 11	R	S	S	S	R	R	S	S	S	R	–	S	–
	S 12	R	S	S	S	R	R	S	R	R	S	–	R	–
	S 13	R	S	S	R	R	R	S	R	R	S	–	R	–
	S 14	R	S	S	S	S	R	S	S	R	R	–	S	–
	S 15	R	S	S	S	R	S	S	S	S	R	–	R	–
	S 16	R	R	S	S	R	R	S	R	R	R	–	R	–
S. aureus	S 17	S	R	–	S	S	R	–	–	–	S	S	–	R
E. coli	S 18	R	S	S	S	R	R	S	R	R	S	–	S	–
	S 19	R	S	S	S	R	R	S	R	R	R	–	R	–
	S 20	R	R	S	S	R	R	S	R	R	R	–	R	–
	S 21	R	S	S	S	R	S	S	R	S	R	–	R	–
	S 22	R	S	S	S	S	S	S	S	S	S	–	S	–
	S 23	S	S	S	S	S	S	S	S	S	S	–	S	–

Table 2. Antibiotic susceptibility of clinical isolates.

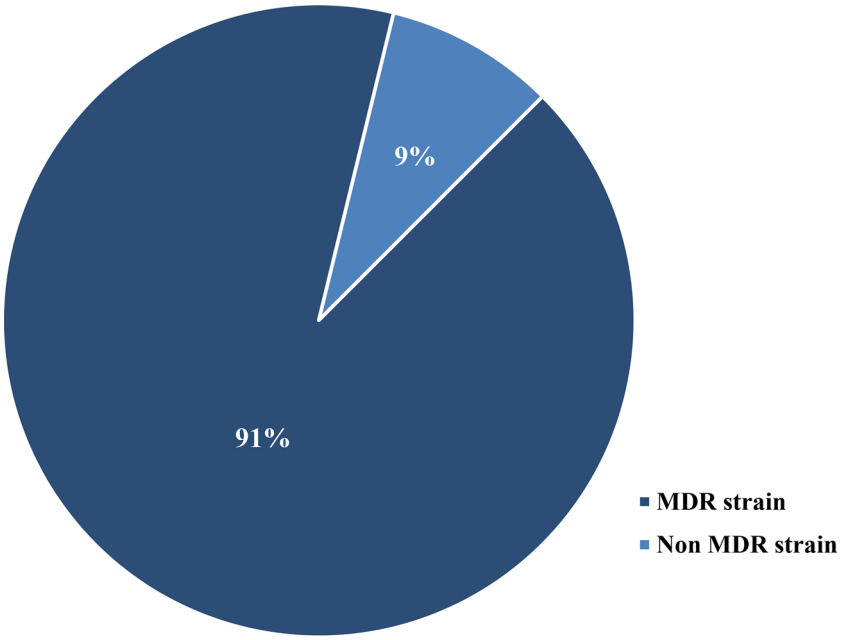

Fig. 7. Percentage of MDR and Non-MDR strains among the twenty-three clinical isolates.

Sample	MIC of CS-AgNPs (µg/ml)	MIC of CTX (µg/ml)
S-01	6.25	–
S-02	3.125	–
S-03	12.5	–
S-04	3.125	125
S-05	6.25	Sensitive to all conc
S-06	3.125	125
S-07	3.125	–
S-08	6.25	–
S-09	12.5	–
S-10	3.125	250
S-11	6.25	250
S-12	–	–
S13	12.5	–
S-14	6.25	500
S-15	3.125	125
S-16	3.125	125
S-17	3.125	Sensitive to all conc
S-18	12.5	–
S-19	6.25	250
S-20	12.5	500
S-21	3.125	250

Table 3. Minimum Inhibitory concentration (MIC) of CS-AgNPs and Cefotaxime (CTX).

Synergism assay of antibiotic CTX in combination with CS-AgNPs

Out of twenty-one isolates, only ten isolates (S-04, S-06, S-10, S-11, S-14, S-15, S-16, S-19, S-20 and S-21) were selected for synergism assay because these isolates showed MIC for both antibiotic and CS-AgNPs. In these ten isolates, five isolates S-11, S-14, S16, S-19 and S-20 showed synergistic effect by obtaining 0.162–0.402 FIC range and the remaining five isolates (S-04, S-06, S-10, S-15, and S-21) showed additive effect with 0.644–0.804 FIC range. Table 4 shows the outcome of synergism assay when antibiotic CTX was used in combination with CS-AgNPs. The significant result of combination might be due to the greater surface area provided by AgNPs that allow the interaction with the amide and hydroxyl groups of antibiotic molecule ultimately leading to the

Sample	MIC (µg/ml)				FIC	Effect
			Combination			
	CS-AgNPs	CTX	AgNPs	CTX		
S-04	3.125	125	2	1	0.648	Additive
S-06	3.125	125	2.5	0.5	0.804	Additive
S-10	3.125	250	2	1	0.644	Additive
S-11	6.25	250	2.5	0.5	0.402	Synergistic
S-14	6.25	500	2.5	0.5	0.401	Synergistic
S-15	3.125	125	2	1	0.648	Additive
S-16	3.125	125	1	2	0.336	Synergistic
S-19	6.25	250	2.5	0.5	0.402	Synergistic
S-20	12.5	500	2	1	0.162	Synergistic
S-21	3.125	250	2.5	0.5	0.802	Additive

Table 4. Synergism assay of antibiotic combination with CS-AgNPs.

disruption of cell wall[59]. Additionally, the positive charges on AgNPs combined with CTX inhibit and disturb the synthesis of cell wall. Ag^{+} ions penetrate the cell and damage the DNA molecule[60].

Antibiofilm activity of CS-AgNPs

Five clinical isolates that showed synergistic effect were used in the antibiofilm assay. The combined effect of CS-AgNPs and CTX on biofilm were analyzed by biofilm inhibition and biofilm eradication assays.

Biofilm inhibition assay

The combination of CS-AgNPs and CTX demonstrated 80–85% biofilm inhibition in three out of five isolates (S-11, S-14, and S-20). In S-11, significant ($p \leq 0.001$) inhibition of biofilm was observed by all treatment combinations in comparison to the untreated group (control). The biofilm inhibition by combination 1 was higher in comparison to the other treatment combinations as depicted in Fig. 8a. Sample S-14 also demonstrated significant ($p \leq 0.001$) inhibition of biofilm formation in response to all tested combinations in comparison to control and among all the combinations, comb 1 showed higher biofilm inhibition as shown in Fig. 8b. Sample S-16 showed 76% biofilm inhibition, which was statistically significant ($p \leq 0.001$) relative to the control. Whereas biofilm inhibition by combination 1, 2, 3 and 4 were more higher in comparison to the remaining groups as shown in Fig. 8c. Sample S-19 showed 68% biofilm inhibition which was statistically significant ($p \leq 0.001$) in comparison to the control group and among all combinations groups, the maximum inhibition was observed in combination 5 as shown in Fig. 8d. All tested combinations against S-20 also showed significant inhibition ($p \leq 0.001$) in contrast to the control group and there was no significant difference between the different combination groups as shown in Fig. 8e.

The mechanism behind the AgNPs antibiofilm potential may be the interference of AgNPs with the early adherence of bacteria towards the surfaces that hinders the biofilm formation. Another factor is that AgNPs may attach to the cell wall of bacteria, avoiding the attachment of bacteria to surfaces which leads to the inhibition of biofilm development. Likewise, AgNPs enter inside the bacterial cell and interrupt the cellular process which are essential in the expansion and maintenance of the biofilm[61] (See Fig. 9).

Biofilm eradication assay

Out of five samples, only S-16 showed 70% biofilm disruption, and four samples (S-11, S-14, S-19, and S-20) did not show any biofilm eradication. When compared to the control group, S-16 showed significant ($p \leq 0.001$) biofilm eradication. Whereas, the comparison of different combinations showed significant ($p \leq 0.001$) biofilm eradication (60–77%) in combination 1, 2, 3, 4 and 5, in comparison to the combination 6 and 7 as shown in the Fig. 10. These findings suggest that the CS-AgNPs have therapeutic potential towards MDR isolates.

Conclusion

The present study demonstrates the synergistic antibacterial and antibiofilm potential of silver nanoparticles against Multi drug resistant bacteria (MDR). CS-AgNPs were synthesized using *Citrus Sinensis* peel extract. ThePlackett-Burman Design showed that the Incubation time, temperature, and ratio of extract to silver nitrate were the significant factors that influence the CS-AgNPs fabrication. Characterization by UV–Vis spectroscopy showed a peak at 470 nm, with particle sizes ranging from 50 to 60 nm. FTIR analysis revealed the involvement of ether, phenol and carboxyl groups in the reduction and stabilization of biosynthesized CS-AgNPs. The biosynthesized CS-AgNPs exhibited significant antibacterial and antibiofilm activity in combination with cefotaxime against MDR clinical isolates, highlighting their potential as a therapeutic option for treating MDR infections.

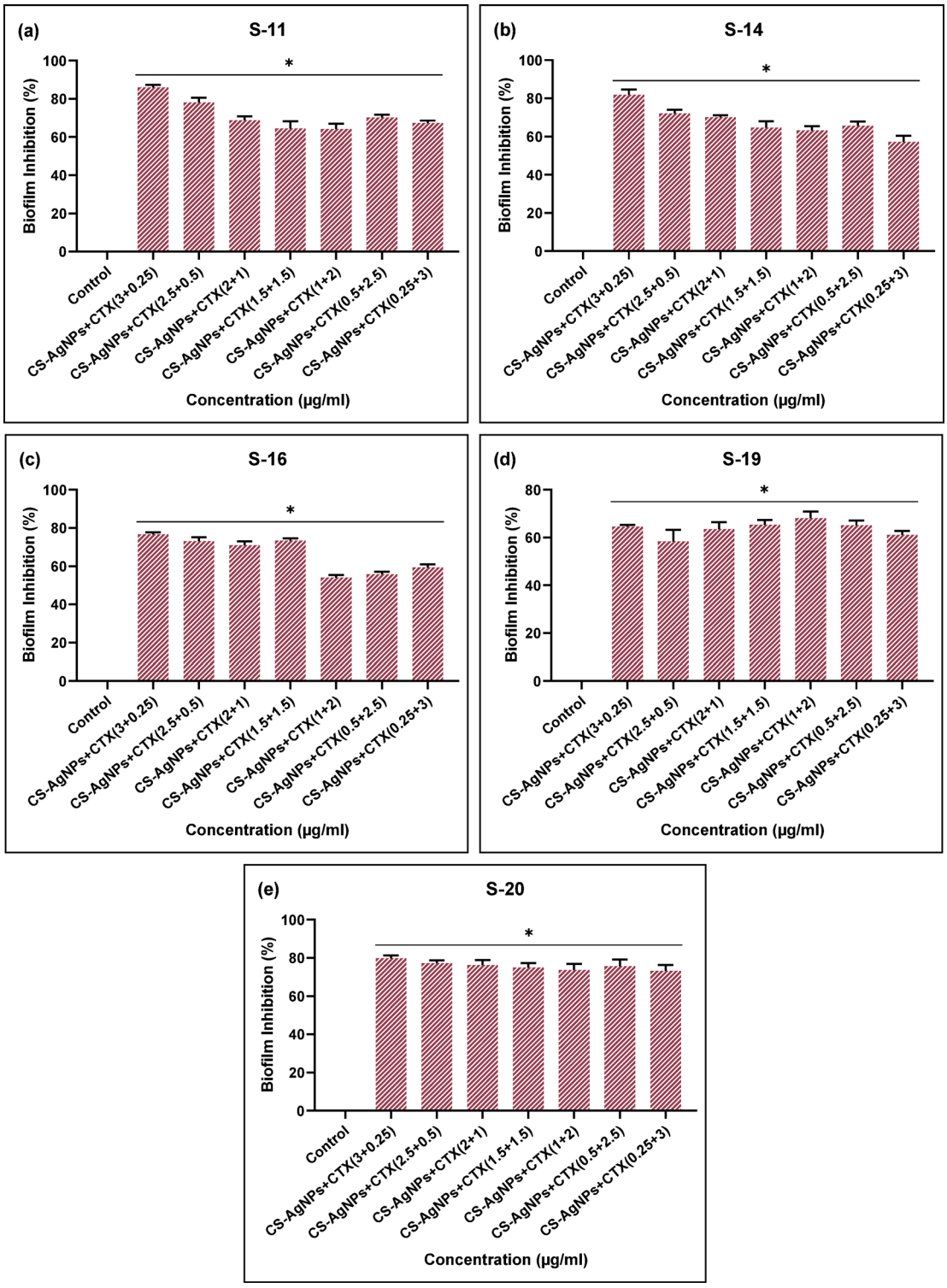

Fig. 8. Biofilm Inhibition Activity. The graphs show the synergistic effect of CS-AgNPs and CTX against biofilm of clinical isolates (**a**) S-11 (**b**) S-14 (**c**) S-16 (**d**) S-19 (**e**) S-20. $^{*}p \leq 0.001$.

Materials and methods

Chemicals and reagents

Silver nitrate was obtained from Dae-Jung Chemical Co., South Korea. Ethanol was acquired from BDH Laboratory Supplies. Nutrient broth, Eosin Methylene Blue (EMB) media, Mueller Hinton Agar (MHA), MacConkey media, Mannitol Salt Agar (MSA) media and antibiotic Ampicillin (10 µg), Amoxiclave (30 µg), Amikacin (30 µg), Gentamicin (10 µg), Cefixime (5 µg), Ciprofloxacin (5 µg), Imipenum (10 µg), Ceftriaxone (30 µg), Norfloxacin (10 µg), Cefotaxime (30 µg), Azithromycin (15 µg), Trimethoprim (10 µg) and Vancomycin (30 µg)

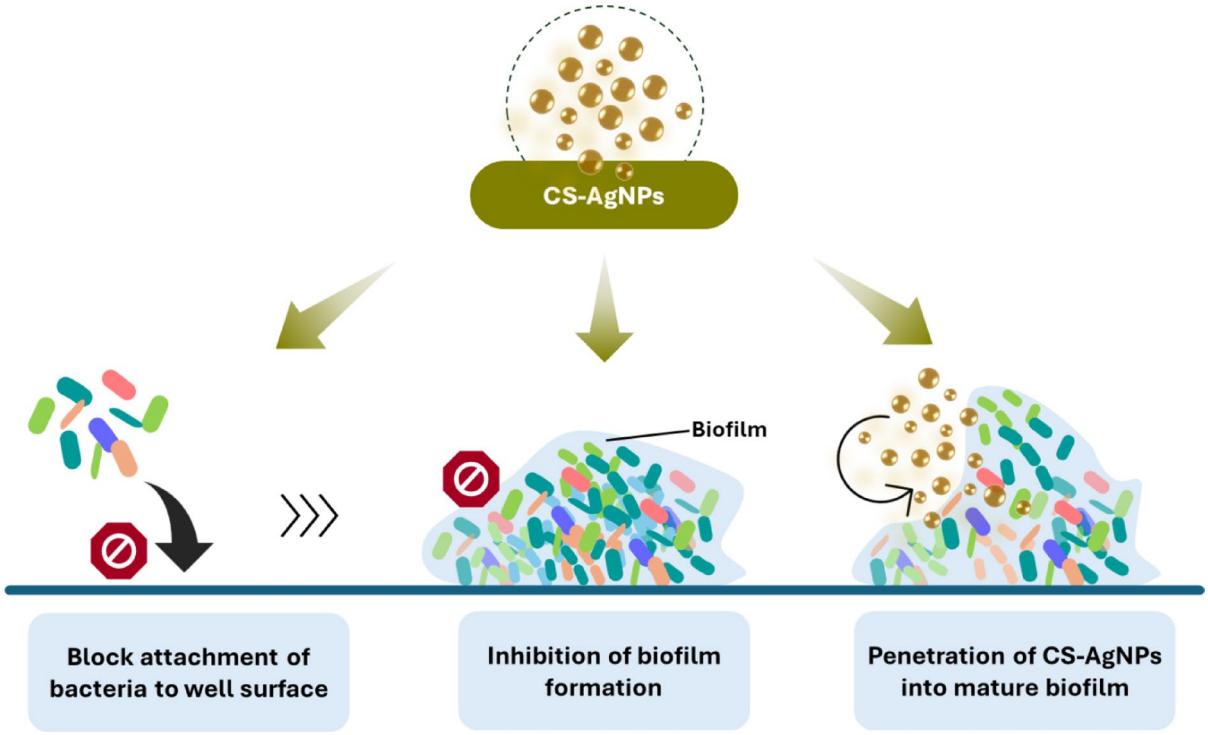

Fig. 9. Biofilm inhibition mechanisms of CS-AgNPs.

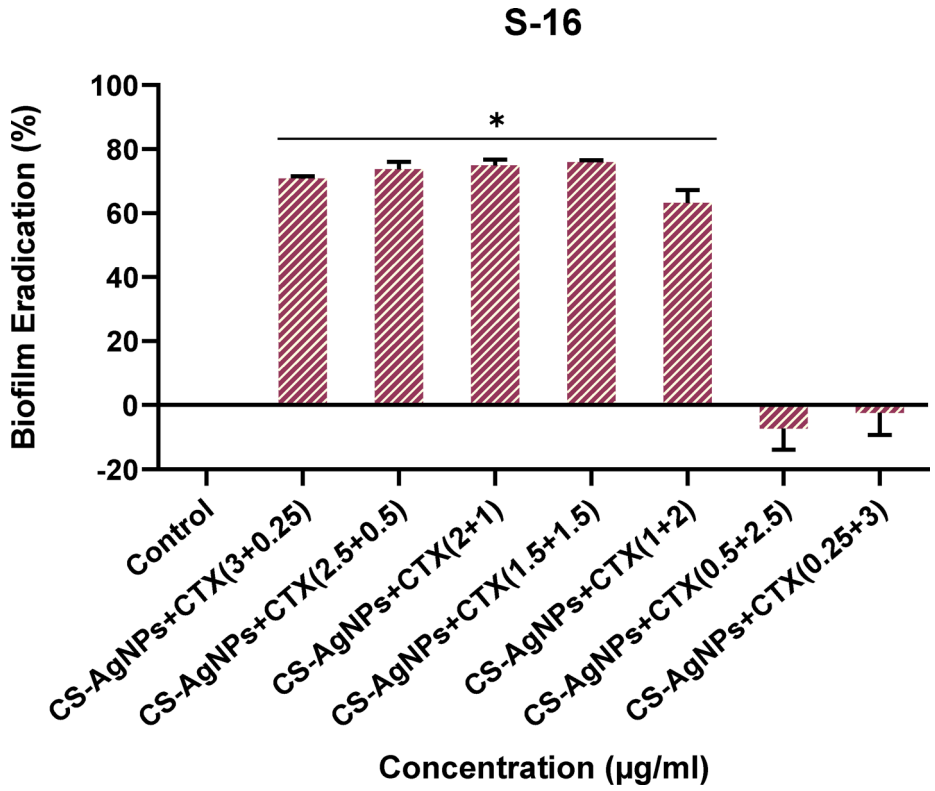

Fig. 10. Biofilm Eradication activity. The graph represents the synergistic effect of CS-AgNPs and CTX on biofilm eradication against S-16 clinical isolate.

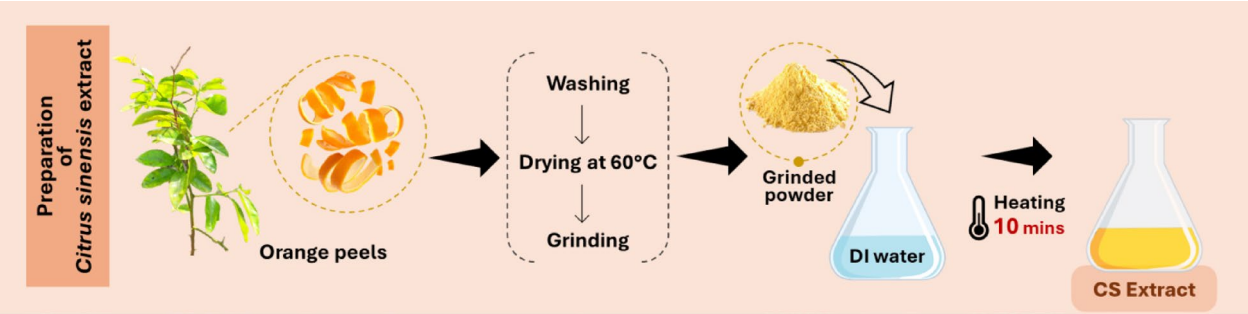

Fig. 11. Pictorial representation of *Citrus sinensis* peel extract preparation.

Parameters	Low	High	Center
Temperature (°C)	30	50	40
Incubation Time (hours)	0.5	4	2.25
$AgNO_3$ Conc. (mM)	1	5	3
Ratio of CS Extract to $AgNO_3$	1:1	1:10	1:5.5

Table 5. Parameters of PBD Experiment for Synthesis of *Citrus sinensis* mediated Silver Nanoparticles.

discs were procured from Oxoid. Dulbecco's Modified Eagle's Medium (DMEM 1X) (Cat:11965092), TryplE (1X) (Cat:12563-011), Trypan blue (0.4%) (Cat:15,250–061), and Fetal Bovine Serum (FBS) (Cat:10500064) were obtained from Gibco (Life Technologies Corp. USA). L-Glutamine (200 mM) (Cat:G7513) was acquired from Sigma. 3-[4,5-dimethylthiazol-2-yl]-2,5 diphenyl tetrazolium bromide (MTT) dye (Cat:A600799) was purchased from BBI life sciences. All chemicals and reagents used in the study were of analytical grade.

Preparation of *Citrus sinensis* (CS) extract

The fruits of *Citrus sinensis* were purchased from the local market in Karachi, Pakistan. To prepare the extract, the peels of *Citrus sinensis* (CS) were thoroughly washed with water. The peels were dried at 60 °C and grinded to form a fine powder. In a 250 ml flask, 5 g of grinded powder was then added to 100 ml deionized (DI) water and the solution was heated up to boiling for 10 min. Following this, the CS extract was obtained by filtering the solution with filter paper[62] (See Fig. 11).

Optimization of *Citrus sinensis* mediated silver nanoparticles (CS-AgNPs) using Plackett–Burman design

The synthesis of silver nanoparticles using *Citrus sinensis* peel extract was optimized using design of experiment (Plackett–Burman design) on Minitab 21. A total of four factors were assessed in the study and each factor was analyzed at two distinct levels: low and high[63,64], as indicated in Table 5. All parameters were run in triplicates and total 39 runs were obtained each showing different combination of factors as shown in Table 6. Each parameter was independent and capable of being characterized by a first-order model according to Plackett–Burman design (PBD).

$$Y = \beta 0 + \sum \beta i + Xi$$

where Y = predicted target response, βi = the regression coefficient, β0 = the model intercept, Xi = an independent parameter.

Characterization of *Citrus sinensis* mediated silver nanoparticles

UV–Vis spectroscopy

According to the parameters in the PBD given in Table 6, the reaction between silver nitrate and *Citrus sinensis* extract was carried out. After reaction completion, UV–Vis spectra (200–800 nm) of the solution were analyzed. Absorption band was observed which indicated the nanoparticle formation[65].

Scanning electron microscopy (SEM) and energy dispersive X-ray spectroscopy (EDX)

Scanning Electron Microscopy was used to identify the structure and size of the CS-AgNPs. The nanoparticle solution was centrifuged, and the pellet was dissolved in DI water. A single drop was placed onto a glass cover slip and allowed to air dry at room temperature. The presence and composition of elements in NPs was identified by SEM–EDX (JEOL JSM-IT100, Japan)[65].

Run order	Incubation temperature	$AgNO_3$ concentration	Incubation time	Ratio of CS extract to $AgNO_3$
1	50	5	0.5	10
2	50	1	0.5	1
3	50	1	4	10
4	50	1	4	1
5	30	5	4	10
6	50	1	4	1
7	50	5	0.5	10
8	30	1	0.5	1
9	30	1	0.5	1
10	30	5	4	10
11	30	1	4	10
12	30	5	0.5	1
13	50	1	4	1
14	30	5	4	10
15	50	1	0.5	1
16	50	1	0.5	1
17	50	5	0.5	10
18	30	1	4	10
19	30	5	4	1
20	50	5	0.5	10
21	50	5	4	1
22	30	5	0.5	1
23	50	1	4	10
24	40	3	2.25	5.5
25	30	5	4	1
26	40	3	2.25	5.5
27	30	1	0.5	1
28	40	3	2.25	5.5
29	50	1	4	10
30	30	5	0.5	1
31	30	1	0.5	10
32	30	1	4	10
33	50	5	4	1
34	50	5	4	1
35	50	5	0.5	10
36	30	1	0.5	10
37	30	1	0.5	10
38	30	5	4	1
39	50	5	0.5	10

Table 6. Plackett–Burman design.

Fourier transform infrared spectroscopy (FTIR)
FTIR was performed to identify the presence of specific functional groups on the surface of NPs. For this purpose, the nanoparticle sample was centrifuged for 45 min at 10,000 rpm. Subsequently, the pellet was rinsed twice with DI water and once with absolute ethanol. The washed pellet was air dried and the FTIR analysis was performed within the range of 3500–600 cm^{-1}[66].

Cytotoxicity assay

The cytotoxicity of CS-AgNPs, CTX and their synergistic treatment were analyzed using MTT colorimetric assay[67]. The normal human fibroblast BJ cell line (CRL-2522™) procured from American Type Culture Collection (ATCC) was used in the assay. For experimental purpose, the cells were grown in DMEM culture media supplemented with FBS (10%), Pen-Strep antibiotic solution (1%), sodium pyruvate (1%) and L-glutamine (1%) and cultured in humidified incubator (New Brunswick S41i, Eppendorf) at 37 °C and 5% CO_2. The cells at confluence stage were harvested using TrypLE and centrifuged at 1000 rpm for 10 min. The cells were counted using Trypan blue staining method followed by seeding of 10×10^3 cells per well for 24 h in 96-well microtiter plate. Post culture, the cells were subjected to treatment with CS-AgNPs and CTX at different concentrations (0.25–3 µg/mL) as well as their synergistic treatment at concentrations specified in Table 7 for 24 h. At 72 h, the culture media was aspirated, and cells were exposed to MTT dye solution (0.5 mg/mL final concentration

Combination codes	CS-AgNPs (µg/ml)	Cefotaxime (CTX) (µg/ml)
Comb 1	3	0.25
Comb 2	2.5	0.5
Comb 3	2	1
Comb 4	1.5	1.5
Comb 5	1	2
Comb 6	0.5	2.5
Comb 7	0.25	3

Table 7. Concentrations of CS-AgNPs and CTX used in Synergism Assay.

in fresh media), incubated in humidified incubator. After 4 h of incubation, the dye solution was carefully aspirated and DMSO (100 µL) was added to each well and the plate was placed on a plate shaker under dark conditions until complete solubilization of formazan crystals for 5 min. The absorbance was recorded at 540 nm using spectrophotometer (Varioskan™ LUX, Thermo Scientific™) and cytotoxic effect was analyzed by following equation:

$$\%Cytotoxicity = 100 - \left(\frac{OD\ (sample) - Mean\ OD\ (blank)}{Mean\ OD\ (control) - Mean\ OD\ (blank)} \right) \times 100$$

Collection of clinical isolates

Sample size or the number of drug-resistant organisms to be screened was determined with PASS (Power Analysis and Sample Size) software version-11[68]. Power Analysis and Sample Size (PASS) Software Version 11 helps researchers determine the appropriate sample size or evaluate the power of statistical tests. It supports various statistical methods and study designs, ensuring studies are adequately powered to detect meaningful effects. The software provides user-friendly tools for accurate sample size calculations and effect size estimation. The calculated sample size was found to be 23 with the power of test 80% along with a 95% confidence interval. These clinical isolates were obtained from blood and urine specimens. Glycerol stocks of the clinical isolates were prepared in 20% glycerol.

Characterization of the clinical isolates

The 23 clinical isolates were initially processed on selective and differential media. A loopful culture of clinical isolates was grown on MacConkey media, MSA and EMB media and incubated at 37 °C for 24 h. The colonies were selected for microscopy and biochemical characterization which included catalase, coagulase, urease and IMViC tests[69–71].

Antibiotic susceptibility of clinical isolates

All identified strains were screened against different antibiotics to check their susceptibility pattern by Kirby Bauer disc diffusion assay. Overnight grown broth cultures were used in the screening test. Turbidity of the culture was adjusted according to 0.5 McFarland Standard by managing the optical density (OD) in the range of 0.08–0.1. This culture was used to prepare smooth lawn on the Muller Hinton agar (MHA) plate. Antibiotic discs were then placed onto the lawn. Plates were incubated at 37 °C for 24 h. Next, clear zone around each disc was observed and diameter of zone of inhibition was measured to interpret it as sensitive, intermediate and resistant, as per CLSI-2020 guideline[72].

Antimicrobial assays

Minimum inhibitory concentration (MIC) of CS-AgNPs and cefotaxime

The broth microdilution method was used to analyze the MIC of synthesized CS-AgNPs and cefotaxime as per the CLSI 2020 guidelines[73]. A single colony was inoculated in 5 ml nutrient broth and incubated for 24 h at 37 °C in a shaking incubator at 100 rpm. Turbidity of the broth culture was adjusted to 0.5 McFarland by obtaining the optical density in the range of 0.08–0.1[72]. Different concentrations of CS-AgNPs (3.125, 6.25, 12.5 and 25 µg/mL) and CTX (125, 250, 500, and 1000 µg/mL) were examined. Nutrient broth (140 µl) and 50 µl CS-AgNPs of above-mentioned concentrations were added to the wells along with the final addition of 10 µl of culture to all wells except the negative control. The experimental plate was incubated at 37 °C in shaking incubator at 60 rpm for 24 h. After incubation, the plate was observed and the absorbance was measured to identify the MIC of the Cs-AgNPs and CTX[68].

Synergism assay

Synergism assay was conducted using CTX in combination with synthesized CS-AgNPs to determine their synergistic effect by using the checkerboard method[74]. In this assay, 96-well plate method was used and in each well, CTX and CS-AgNPs were added in such a way that each well contained unique concentration of CTX and CS-AgNPs as mentioned in Table 7. The CTX was used in low to high concentration while the CS-AgNPs in high to low concentration. In each well, bacterial culture was added, and OD of the culture was adjusted to 0.5 McFarland. The plates were incubated at 37 °C for 24 h in shaking incubator at 60 rpm. Post incubation period,

turbidity was observed and the absorbance was recorded at 540 nm[72]. The synergistic effect of antibiotic with CS-AgNPs was calculated and reported as Fractional Inhibitory Concentration (FIC).

The synergistic effect was considered if FIC index value was ≤ 0.5, additive if 0.5 < FIC ≤ 1, indifferent if 1 < FIC < 2 and antagonistic if FIC ≥ 2[75].

FICI was calculated with the help of the following formula[75].

$$FIC\ index = FIC_{\mathrm{a}} + FIC_{b} = \frac{MIC_{\mathrm{a}}\ in\ combination}{MIC_{\mathrm{a}}\ alone} + \frac{MIC_{\mathrm{b}}\ in\ combination}{MIC_{\mathrm{b}}\ alone}$$

where a is AgNPs and b is Antibiotic (Cefotaxime).

Antibiofilm assays

Cultures with the synergistic effect were used in the antibiofilm assay. The synergistic effect of CS-AgNPs and CTX on biofilm were analyzed by biofilm inhibition and biofilm disruption assays.

Biofilm inhibition assay

The synergistic effects of CS-AgNPs and CTX on biofilm formation was evaluated by using crystal violet method[76]. Firstly, 140 µl nutrient broth was added in the wells followed by the addition of 10 µl culture (optical density between 0.08 and 1.0). CS-AgNPs and antibiotic concentration used in the synergism assay is mentioned in Table 7. The negative and positive control wells contained only nutrient broth and culture, respectively. The plates were incubated at 37 °C for 24 h. After incubation, the planktonic cells were removed without disturbing the biofilm and the wells were washed twice with distilled water. Post washing, 0.1% crystal violet was added to the wells and incubated at 37 °C at 70 rpm for 20 min. The wells were then rinsed with distilled water and allowed to dry. The biofilm was solubilized by adding 200 µl of 95% ethanol followed by incubation for 10 min at room temperature. After incubation, the solution was transferred into the sterile 96-well plate and the absorbance readings were recorded at 590 nm[75].

Biofilm eradication assay

Flat bottom 96-well plates were used in this assay. 190 µl nutrient broth was added in the wells along with 10 µl tested culture (at 0.08–0.1 OD), positive control (200 µl culture) and negative control (nutrient broth only) were incubated for 24 h at 37 °C. Following incubation, the plate was rinsed twice with distilled water and air dried. In dried plate, the nutrient broth (150 µl), was added followed by addition of CS-AgNPs and CTX in a concentration used in the synergism assay. The plate was rinsed twice, and the biofilm was stained with 0.1% crystal violet followed by incubation for 20 min at 37 °C at 70 rpm. Post incubation, the wells were rinsed with distilled water and allowed to air dry. The biofilm was solubilized by the addition of 200 µl of 95% ethanol and incubated for 10 min. After incubation, the solution was transferred to the sterile 96-well plate and the absorbance was measured at 590 nm[75]. The percent biofilm inhibition or disruption was calculated using the below-mentioned formula:

$$Percent\ biofilm\ inhibition\ or\ disruption = \left(\frac{A_{590nm}\ without\ AgNPs\ -\ A_{590nm}\ with\ AgNPs}{A_{590nm}\ without\ AgNPs}\right) \times 100$$

where A = Absorbance.

Statistical analysis

The resulted data was analyzed statistically with SPSS software (version-22). One way ANOVA followed by Tukey's post hoc test was used for statistical significance and $p \leq 0.05$ was considered statistically significant. The graphical representation was done with GraphPad Prism software (version-8). All the results were represented as mean ± standard error of mean (SEM).

Data availability

Data is provided within the manuscript.

Received: 3 October 2024; Accepted: 6 May 2025
Published online: 28 May 2025

References

1. Murray, C. J. et al. Global burden of bacterial antimicrobial resistance in 2019: a systematic analysis. *The lancet* **399**, 629–655. https://doi.org/10.1016/S0140-6736(21)02724-0 (2022).
2. Laxminarayan, R. et al. The lancet infectious diseases commission on antimicrobial resistance: 6 years later. *Lancet Infect. Dis.* **20**, e51–e60. https://doi.org/10.1016/s1473-3099(20)30003-7 (2020).
3. Menichetti, A., Mavridi-Printezi, A., Mordini, D. & Montalti, M. Effect of size, shape and surface functionalization on the antibacterial activity of silver nanoparticles. *J. Funct. Biomater.* **14**, 244. https://doi.org/10.3390/jfb14050244 (2023).
4. Planquette, B. et al. Pseudomonas aeruginosa ventilator-associated pneumonia. predictive factors of treatment failure. *Am. J. Respir. Crit. Care Med.* **188**, 69–76. https://doi.org/10.1164/rccm.201210-1897OC (2013).
5. Bayeh Abera, B. A., Mulugeta Kibret, M. K. & Wondemagegn Mulu, W. M. Knowledge and beliefs on antimicrobial resistance among physicians and nurses in hospitals in Amhara Region, Ethiopia. *BMC Pharmacol. Toxicol.* https://doi.org/10.1186/2050-6511-15-26 (2014).
6. Khan, S. N. & Khan, A. U. Breaking the spell: Combating multidrug resistant 'superbugs'. *J. Front. Microbiol.* **7**, 174. https://doi.org/10.3389/fmicb.2016.00174 (2016).

7. Qayyum, S. & Khan, A. U. Nanoparticles versus biofilms: A battle against another paradigm of antibiotic resistance. *J. MedChemComm* **7**, 1479–1498. https://doi.org/10.1039/C6MD00124F (2016).
8. Huh, A. J. & Kwon, Y. J. "Nanoantibiotics": A new paradigm for treating infectious diseases using nanomaterials in the antibiotics resistant era. *J. Control. Release* **156**, 128–145. https://doi.org/10.1016/j.jconrel.2011.07.002 (2011).
9. Costerton, J. W., Stewart, P. S. & Greenberg, E. P. Bacterial biofilms: A common cause of persistent infections. *Science* **284**, 1318–1322. https://doi.org/10.1126/science.284.5418.1318 (1999).
10. Stewart, P. S. Diffusion in biofilms. *J. Bacteriol.* **185**, 1485–1491. https://doi.org/10.1128/JB.185.5.1485-1491.2003 (2003).
11. Hamzeh, M. & Sunahara, G. I. In vitro cytotoxicity and genotoxicity studies of titanium dioxide (TiO2) nanoparticles in Chinese hamster lung fibroblast cells. *Toxicol. In Vitro* **27**, 864–873. https://doi.org/10.1016/j.tiv.2012.12.018 (2013).
12. Wang, L., Hu, C. & Shao, L. The antimicrobial activity of nanoparticles: Present situation and prospects for the future. *Int. J. Nanomed.* **12**, 1227–1249. https://doi.org/10.2147/IJN.S121956 (2017).
13. Habash, M. B. et al. Potentiation of tobramycin by silver nanoparticles against Pseudomonas aeruginosa biofilms. *Antimicrob. Agents Chemother.* **61**, 00415–00417. https://doi.org/10.1128/AAC.00415-17 (2017).
14. Naganathan, K. & Thirunavukkarasu, S. Green way genesis of silver nanoparticles using multiple fruit peels waste and its antimicrobial, anti-oxidant and anti-tumor cell line studies. *IOP Conf. Ser.: Mater. Sci. Eng.* **191**, 012009. https://doi.org/10.1088/1757-899X/191/1/012009 (2017).
15. Baptista, P. V. et al. Nano-strategies to fight multidrug resistant bacteria: "A Battle of the Titans". *J. Front. Microbiol.* **9**, 1441. https://doi.org/10.3389/fmicb.2018.01441 (2018).
16. Altinsoy, B. D., Karatoprak, G. Ş & Ocsoy, I. Extracellular directed ag NPs formation and investigation of their antimicrobial and cytotoxic properties. *Saudi Pharm. J.* **27**, 9–16. https://doi.org/10.1016/j.jsps.2018.07.013 (2019).
17. Ansar, S. et al. Eco friendly silver nanoparticles synthesis by Brassica oleracea and its antibacterial, anticancer and antioxidant properties. *Sci. Rep.* **10**, 18564. https://doi.org/10.1038/s41598-020-74371-8 (2020).
18. Mostafavi, E. et al. Antineoplastic activity of biogenic silver and gold nanoparticles to combat leukemia: Beginning a new era in cancer theragnostic. *Biotechnol Rep. (Amst)* **34**, e00714. https://doi.org/10.1016/j.btre.2022.e00714 (2022).
19. Rai, M., Yadav, A. & Gade, A. Silver nanoparticles as a new generation of antimicrobials. *J. Biotechnol. Adv.* **27**, 76–83. https://doi.org/10.1016/j.biotechadv.2008.09.002 (2009).
20. Abbate, L. et al. Genetic improvement of Citrus fruits: New somatic hybrids from *Citrus sinensis* (L.) Osb. and Citrus limon (L.) Burm F.. *J. Food Res. Int.* **48**, 284–290. https://doi.org/10.1016/j.foodres.2012.04.007 (2012).
21. Gupta, S., Choudhary, D. K. & Sundaram, S. Green synthesis and characterization of silver nanoparticles using *Citrus sinensis* (Orange peel) extract and their antidiabetic, antioxidant, antimicrobial and anticancer activity. *Waste Biomass Valor.* **16**, 1101–1114. https://doi.org/10.1007/s12649-024-02782-z (2025).
22. Khabeeri, O. M., Al-Thabaiti, S. A. & Khan, Z. Citrus sinensis peel waste assisted synthesis of AgNPs: effect of surfactant on the nucleation and morphology. *SN Appl. Sci.* **2**, 2038. https://doi.org/10.1007/s42452-020-03801-z (2020).
23. Kaviya, S., Santhanalakshmi, J., Viswanathan, B., Muthumary, J. & Srinivasan, K. Biosynthesis of silver nanoparticles using citrus sinensis peel extract and its antibacterial activity. *Spectrochim. Acta Part A: Mol. Biomol. Spectrosc.* **79**, 594–598. https://doi.org/10.1016/j.saa.2011.03.040 (2011).
24. Singh, A. et al. Green synthesis of metallic nanoparticles as effective alternatives to treat antibiotics resistant bacterial infections: A review. *J. Biotechnol. Rep.* **25**, e00427. https://doi.org/10.1016/j.btre.2020.e00427 (2020).
25. Ferdous, Z. & Nemmar, A. Health impact of silver nanoparticles: A review of the biodistribution and toxicity following various routes of exposure. *Int. J. Mol. Sci.* **21**, 2375. https://doi.org/10.3390/ijms21072375 (2020).
26. Ali, H. R., Emam, A. N., Koraney, N. F., Hefny, E. G. & Ali, S. F. Combating the prevalence of water-borne bacterial pathogens using anisotropic structures of silver nanoparticles. *J. Nanopart. Res.* **22**, 1–15. https://doi.org/10.1007/s11051-020-4760-6 (2020).
27. Fahim, M. et al. Green synthesis of silver nanoparticles: A comprehensive review of methods, influencing factors, and applications. *JCIS Open* **16**, 100125. https://doi.org/10.1016/j.jciso.2024.100125 (2024).
28. Tyagi, R. et al. Application of design of experiment (DoE) for optimization of multiple parameter resource constrain process: Taguchi-based fractional factorial approach. *Adv. J. Chem.* **6**, 391–400. https://doi.org/10.48309/ajca.2023.405974.1381 (2023).
29. Farooq, M. A., Nóvoa, H., Araújo, A. & Tavares, S. M. An innovative approach for planning and execution of pre-experimental runs for Design of Experiments. *Eur. Res. Manag. Bus. Econ.* **22**, 155–161. https://doi.org/10.1016/j.iedee.2014.12.003 (2016).
30. Zhou, J. et al. Optimization of phenol degradation by Candida tropicalis Z-04 using Plackett–Burman design and response surface methodology. *J. Environ. Sci. (China)* **23**, 22–30. https://doi.org/10.1016/s1001-0742(10)60369-5 (2011).
31. Gorinstein, S. et al. Comparison of some biochemical characteristics of different citrus fruits. *J. Food Chem.* **74**, 309–315. https://doi.org/10.1016/S0308-8146(01)00157-1 (2001).
32. Sheik, G. B., Abdel, R., Alzeyadi, Z. A. & AlGhonaim, M. I. Application of Plackett–Burman design for optimization of silver nanoparticles produced by Streptomyces sp. DW102. *Int. J. Adv. Biotechnol. Res.* **10**, 143–151 (2019).
33. World Health, O. & Resistance, W. H. O. *Critically Important Antimicrobials for Human Medicine: Ranking of Antimicrobial Agents for Risk Management of Antimicrobial Resistance Due to Non-Human Use*. 5th rev. edn, 48 p. (World Health Organization, 2017).
34. Giske, C. G. et al. Redefining extended-spectrum β-lactamases: balancing science and clinical need. *J. Antimicrob. Chemother.* **63**, 1–4. https://doi.org/10.1093/jac/dkn444 (2008).
35. National Antimicrobial Resistance (AMR) Surveillance Report Pakistan 2021–2022. (National Institute of Health, Pakistan).
36. Laime-Oviedo, L. A. et al. Optimization of synthesis of silver nanoparticles conjugated with *Lepechinia meyenii* (Salvia) Using Plackett–Burman design and response surface methodology—preliminary antibacterial activity. *J. Processes* **10**, 1727. https://doi.org/10.3390/pr10091727 (2022).
37. Ali, M. et al. Green synthesis and characterization of silver nanoparticles using *Artemisia absinthium* aqueous extract: A comprehensive study. *Mater. Sci. Eng.: C* **58**, 359–365. https://doi.org/10.1016/j.msec.2015.08.045 (2016).
38. Rodríguez-León, E. et al. Synthesis of silver nanoparticles using reducing agents obtained from natural sources (*Rumex hymenosepalus* extracts). *J. Nanoscale Res. Lett.* **8**, 1–9. https://doi.org/10.1186/1556-276X-8-318 (2013).
39. Zannotti, M., Piras, S., Magnaghi, L. R., Biesuz, R. & Giovannetti, R. Silver nanoparticles from orange peel extract: Colorimetric detection of Pb2+ and Cd2+ ions with a chemometric approach. *Spectrochim. Acta Part A: Mol. Biomol. Spectrosc.* **323**, 124881. https://doi.org/10.1016/j.saa.2024.124881 (2024).
40. Mickky, B., Elsaka, H., Abbas, M., Gebreil, A. & Shams Eldeen, R. Orange peel-mediated synthesis of silver nanoparticles with antioxidant and antitumor activities. *BMC Biotechnol.* **24**, 66. https://doi.org/10.1186/s12896-024-00892-z (2024).
41. Das, R. et al. Green synthesis of silver nanoparticles using *Trema Orientalis* (L.) extract and evaluation of their antibacterial activity. *Green Chem. Lett. Rev.* **18**, 2444679. https://doi.org/10.1080/17518253.2024.2444679 (2025).
42. Kumar, P. et al. Efficient catalytic degradation of selected toxic dyes by green biosynthesized silver nanoparticles using aqueous leaf extract of cestrum nocturnum L.. *Nanomaterials* **12**, 3851 (2022).
43. Chen, B. B., Liu, H., Huang, C. Z., Ling, J. & Wang, J. Rapid and convenient synthesis of stable silver nanoparticles with kiwi juice and its novel application for detecting protease K. *N. J. Chem.* **39**, 1295–1300. https://doi.org/10.1039/C4NJ01578A (2015).
44. Mittal, J., Singh, A., Batra, A. & Sharma, M. M. Synthesis and characterization of silver nanoparticles and their antimicrobial efficacy. *J Part. Sci. Technol.* **35**, 338–345 (2017).
45. Skiba, M. I. & Vorobyova, V. I. Synthesis of silver nanoparticles using orange peel extract prepared by plasmochemical extraction method and degradation of methylene blue under solar irradiation. *Adv. Mater. Sci. Eng.* **2019**, 8306015. https://doi.org/10.1155/2019/8306015 (2019).

46. Ibrahim, H. M. Green synthesis and characterization of silver nanoparticles using banana peel extract and their antimicrobial activity against representative microorganisms. *J. Radiat. Res. Appl. Sci.* **8**, 265–275. https://doi.org/10.1016/j.jrras.2015.01.007 (2015).
47. Mahrous, S. S., Galil, E. A. & Mansy, M. S. Investigation of modified orange peel in the removal of Cd2+, Co2+ and Zn2+ from wastewater. *J. Radioanal. Nucl. Chem.* **331**, 985–997. https://doi.org/10.1007/s10967-021-08166-0 (2022).
48. Rathinavel, S. & Saravanakumar, S. Synthesis of silver nanoparticles through orange peel powder for antibacterial composite filler applications. *J. Polym. Environ.* https://doi.org/10.1007/s10924-021-02276-2 (2022).
49. ISO 10993–5:2009 Biological evaluation of medical devices—Part 5: Tests for in vitro cytotoxicity. (2009).
50. Khursheed, N., Mal, P. B. & Taimoor, M. Frequency of isolation and susceptibility pattern of *E. coli* from in and outpatients over a period of five years at The Indus Hospital Network, Karachi Pakistan. *J. Pakistan Med. Assoc.* **70**, 1587–1590. https://doi.org/10.5455/JPMA.2253 (2020).
51. Saleem, Z., Hassali, M. A. & Hashmi, F. K. Pakistan's national action plan for antimicrobial resistance: Translating ideas into reality. *Lancet infect. Dis.* **18**, 1066–1067. https://doi.org/10.1016/S1473-3099(18)30516-4 (2018).
52. Breijyeh, Z., Jubeh, B. & Karaman, R. Resistance of gram-negative bacteria to current antibacterial agents and approaches to resolve it. *Molecules* **25**, 1340. https://doi.org/10.3390/molecules25061340 (2020).
53. Singh, P. et al. Green synthesis of gold and silver nanoparticles from *Cannabis sativa* (industrial hemp) and their capacity for biofilm inhibition. *Int. J. Nanomed.* https://doi.org/10.2147/IJN.S157958 (2018).
54. Liao, C., Li, Y. & Tjong, S. C. Bactericidal and cytotoxic properties of silver nanoparticles. *Int. J. Mol. Sci.* **20**, 449. https://doi.org/10.3390/ijms20020449 (2019).
55. Taglietti, A. et al. Antibacterial activity of glutathione-coated silver nanoparticles against gram positive and gram negative bacteria. *J. Langmuir* **28**, 8140–8148. https://doi.org/10.1021/la3003838 (2012).
56. Kędziora, A. et al. Similarities and differences between silver ions and silver in nanoforms as antibacterial agents. *Int. J. Mol. Sci.* **19**, 444. https://doi.org/10.3390/ijms19020444 (2018).
57. Escárcega-González, C. E. et al. In vivo antimicrobial activity of silver nanoparticles produced via a green chemistry synthesis using *Acacia rigidula* as a reducing and capping agent. *Int. J. Nanomed.* **13**, 2349–2363. https://doi.org/10.2147/IJN.S160605 (2018).
58. Onitsuka, S., Hamada, T. & Okamura, H. Preparation of antimicrobial gold and silver nanoparticles from tea leaf extracts. *J. Colloids Surfaces B: Biointerfaces* **173**, 242–248. https://doi.org/10.1016/j.colsurfb.2018.09.055 (2019).
59. Fayaz, A. M. et al. Biogenic synthesis of silver nanoparticles and their synergistic effect with antibiotics: A study against gram-positive and gram-negative bacteria. *J. Nanomed.: Nanotechnol. Biol. Med.* **6**, 103–109. https://doi.org/10.1016/j.nano.2009.04.006 (2010).
60. Rai, M. K., Deshmukh, S., Ingle, A. & Gade, A. Silver nanoparticles: The powerful nanoweapon against multidrug-resistant bacteria. *J. Appl. Microbiol.* **112**, 841–852. https://doi.org/10.1111/j.1365-2672.2012.05253.x (2012).
61. Verduzco-Chavira, K. et al. Antibacterial and antibiofilm activity of chemically and biologically synthesized silver nanoparticles. *J. Antibiotics* **12**, 1084. https://doi.org/10.3390/antibiotics12071084 (2023).
62. Al-Shabib, N. A. et al. Bio-inspired facile fabrication of silver nanoparticles from in vitro grown shoots of *Tamarix nilotica*: Explication of its potential in impeding growth and biofilms of Listeria monocytogenes and assessment of wound healing ability. *RSC Adv.* **10**, 30139–30149. https://doi.org/10.1039/d0ra04587j (2020).
63. Naysmith, A., Mian, N. S. & Rana, S. Green synthesised silver nanocomposite for thermoregulating E-textiles. *J. Eng. Proc.* **15**, 15. https://doi.org/10.3390/engproc2022015015 (2022).
64. Halima, R., Narula, A. & Sravanthi, V. Optimization of process parameters for the green synthesis of silver nanoparticles using Plackett–Burman and 3-level Box–Behnken design. *J. Huazhong Univ. Sci. Technol.* **1671**, 4512 (2021).
65. Choudhary, S. et al. Sustainable phyco-fabrication of silver nanoparticles using *Coelastrella terrestris* and their multiple downstream applications. *Biocatal. Agric. Biotechnol.* **53**, 102854. https://doi.org/10.1016/j.bcab.2023.102854 (2023).
66. Muraro, P. C. L. et al. Silver nanoparticles from residual biomass: Biosynthesis, characterization and antimicrobial activity. *J. Biotechnol.* **343**, 47–51. https://doi.org/10.1016/j.jbiotec.2021.11.003 (2022).
67. van Meerloo, J., Kaspers, G. J. L. & Cloos, J. in *Cancer Cell Culture: Methods and Protocols* (ed Ian A. Cree) 237–245 (Humana Press, 2011).
68. Farooq, U. et al. Rifampicin conjugated silver nanoparticles: A new arena for development of antibiofilm potential against methicillin resistant Staphylococcus aureus and *Klebsiella pneumoniae*. *Int. J. Nanomed.* **14**, 3983–3993. https://doi.org/10.2147/IJN.S198194 (2019).
69. Gholipour, A. et al. Phenotypic and Molecular characterization of extended-spectrum beta-lactamase produced by *Escherichia coli*, and Klebsiella pneumoniae Isolates in an Educational Hospital. *Jundishapur J. Microbiol.* https://doi.org/10.5812/jjm.11758 (2014).
70. Ntuli, V., Njage, P. M. K. & Buys, E. M. Characterization of *Escherichia coli* and other Enterobacteriaceae in producer-distributor bulk milk. *J. Dairy Sci.* **99**, 9534–9549. https://doi.org/10.3168/jds.2016-11403 (2016).
71. Tiwari, H. K. & Sen, M. R. Emergence of vancomycin resistant *Staphylococcus aureus* (VRSA) from a tertiary care hospital from northern part of India. *BMC Infect. Dis.* **6**, 1–6. https://doi.org/10.1186/1471-2334-6-156 (2006).
72. Balto, H., Bukhary, S., Al-Omran, O., BaHammam, A. & Al-Mutairi, B. Combined effect of a mixture of silver nanoparticles and calcium hydroxide against *Enterococcus faecalis* biofilm. *J. Endod.* **46**, 1689–1694. https://doi.org/10.1016/j.joen.2020.07.001 (2020).
73. CLSI. Performance Standards for Antimicrobial Susceptibility Testing, M100 Ed30. (2020).
74. Gupta, A. et al. Synergistic antimicrobial therapy using nanoparticles and antibiotics for the treatment of multidrug-resistant bacterial infection. *J. Nano Fut.* **1**, 015004. https://doi.org/10.1088/2399-1984/aa69fb (2017).
75. Tawre, M. S. et al. Synergistic and antibiofilm potential of *Curcuma aromatica* derived silver nanoparticles in combination with antibiotics against multidrug-resistant pathogens. *Front. Chem.* https://doi.org/10.3389/fchem.2022.1029056 (2022).
76. Gaidhani, S. V. et al. Time dependent enhanced resistance against antibiotics & metal salts by planktonic & biofilm form of *Acinetobacter haemolyticus* MMC 8 clinical isolate. *Indian J. Med. Res.* **140**, 665–671 (2014).

Acknowledgements

We would like to thank Dow University of Health Sciences for providing the facilities to successfully conduct the study. Additionally we would like to express our sincere gratitude to Dr. Saba Farooq for providing her expertise related to synergistic studies.

Author contributions

H.K: Methodology, Investigation, Data curation, Writing—original draft, Writing—review & editing A.G: Conceptualization, Funding acquisition, Methodology, Investigation, Data curation, Writing—review & editing. Z.N: Methodology, Investigation, Data curation, T.M: Investigation, Methodology, Data curation. review.

Declarations

Competing interests
The authors declare no competing interests.

Ethical approval
All the experiments were conducted after getting ethical approval (IRB-3393/DUHS/Exemption/2024/50) from Institutional Review Board of Dow University of Health Sciences, Karachi, Pakistan.

Additional information
Supplementary Information The online version contains supplementary material available at https://doi.org/10.1038/s41598-025-01524-y.

Correspondence and requests for materials should be addressed to A.G.

Reprints and permissions information is available at www.nature.com/reprints.

Publisher's note Springer Nature remains neutral with regard to jurisdictional claims in published maps and institutional affiliations.